Ring-shaped DC Distribution Network Protection Scheme Research Based-on Voltage Prediction

Ring-shaped DC Distribution Network Protection Scheme Research Based-on Voltage Prediction

CHANG Xiao[1], WANG Cheng[2], LIU Yizhao[1], ZHANG Min[1], FAN Rui[1], SHANG Guanxin[2]

Shanxi Electric Power Research Institute, Shan Xi, China
College of Electrical and Power Engineering, Taiyuan University of Technology, Shan Xi, China
N0.79 West Yingze Street, Taiyuan, 030024, Shanxi Province, P.R.China

Mobile: +86-18234179293

E-mail: 1317566471@qq.com

Abstract. In this paper, it researches the DC-ring distribution network protection scheme. Firstly, it analyzes the fault characteristics of the voltage source converter (VSC) during the DC line-to-ground. Secondly, it proposes a DC distribution network protection scheme based-on local measurement. The quadratic time-varying function is utilized to predict the line-side voltage in case of failure. The difference between the predicted voltage and the measured voltage on the line side in case of failure is utilized as the primary protective action criterion. Under voltage protection is utilized as backup protection in DC ring distribution network to guarantee safety and stability in case of failure. And the overcurrent protection is utilized as the startup criterion. The additional criteria are added to the further distinction between internal faults and external faults to prevent protection malfunction. The loop DC-distribution network protection scheme simulation based-on real-time digital simulator (RTDS) has verified the feasibility and effectiveness of the proposed scheme.

1. Introduction

In recent years, with the development of science and technology, the demand for electricity is growing in load-intensity areas. The existing AC power distribution system cannot satisfy the customer's power demand to some extent. However, in the DC distribution network, the control of active power and reactive power on the AC side is independent, and it exists some defects in frequency offset and three-phase asymmetry. So, the DC power distribution system is coming into people's notice [1],[2]. DC power distribution has quickly occupied a place in the power market with its low price, low line loss, large transmission capacity and high reliability [3],[4].

One of the main challenges in adopting the DC distribution system is the lack of a practical solution to the fault protection. Another is the lack of adequate protection responses to DC grid failures. In general, there are three methods, protection based on current and voltage, differential protection and the travelling wave protection [5]. Protection based on current and voltage is widespread at the beginning since the most apparent features of DC faults are the rise of DC and the drop of DC voltage [6]. But the fault characteristics of the current and voltage are very similar when the system has internal or external faults in the ring network. In terms of the selectivity, differential protection is an ideal protection scheme. But information transmission would be time-consuming with

long transmission lines [7]. In the DC faults, the short-circuit current usually peaks the rated current within 10ms, which causes the IGBT to be locked. To prevent power electronics from being damaged, the fault needs to be cut within 10ms [8]. Travelling wave protection has been widely used in the traditional high voltage DC transmission system, and it showed good performances. But the travelling wave is hard to detect especially for low voltage MTDC systems [7]. With the development of DC protection technology, some protection based on DC voltage and the current transient figure is also widely used [9]. Overcurrent is a good indicator of a fault in low-voltage DC distribution systems. However, when a DC line fault occurs with high resistance, the overcurrent is not apparent enough [10]. Both dv/dt method and di/dt method are depended on the fault loop impedance. These methods are sensitive to fault resistance [11].

For all of this, this paper deals with the DC fault protection in VSC-based multi-terminal DC systems. Based on the attenuation characteristic of transient voltage, an effective transient-voltage protection method is proposed to locate fault fast and reliable. In Section 2, the transient voltage and its attenuation characteristic in the DC network are clarified as the research foundation. In Section 3, a quadratic time depended model derives from analog voltage. In Section 4, an effective protection system scheme for a DC distribution network has been proposed in this paper. The verification of the method is presented in Section 5. At last, some conclusions are given in Section 6.

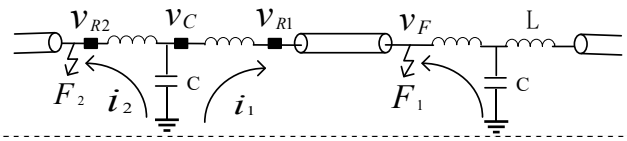

Fig. 1. Faulted network section.

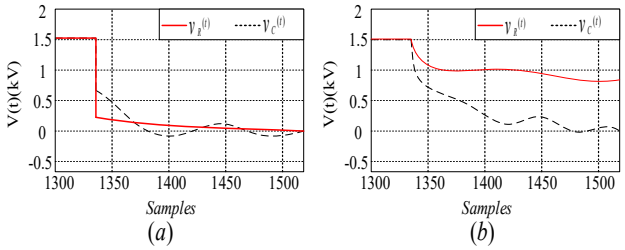

Fig. 2. Plots of v_R and v_C fault F_1.

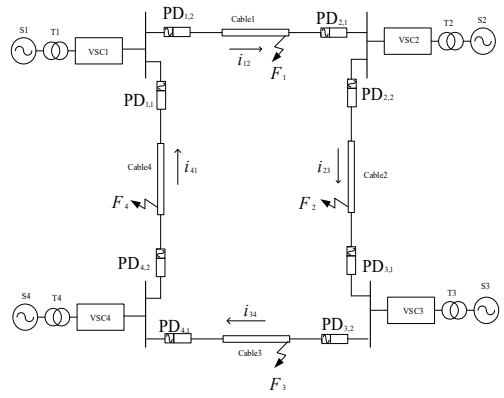

Fig. 3. Faulted network section.

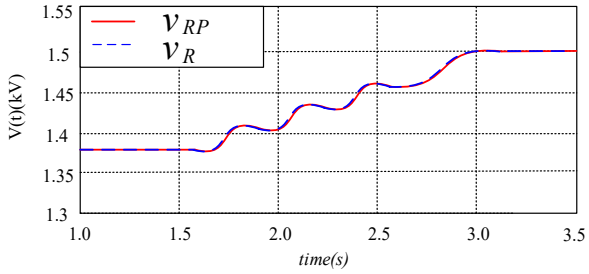

Fig. 4. The waveform of v_{RP} and v_R when power change.

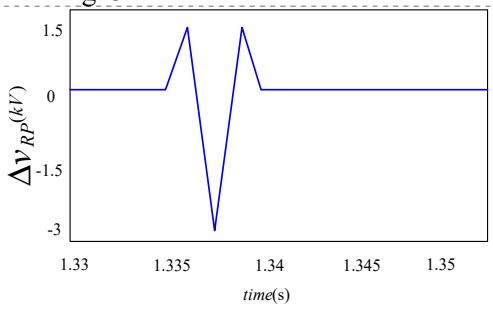

Fig. 5. The waveform diagram of the difference between predicted voltage and measured voltage.

2. SYSTEM ANALYSIS DURING FAULT

The DC distribution network is a small inertia system, by using the control module to maintain the voltage stability of the entire DC ring network. When the system is running stable, the voltage of the whole DC ring network remains unchanged, and the DC fluctuates slightly. When the ground fault occurs, the voltage drops rapidly, and the current rapidly increases, then it will cause the converter locked. In a toroidal DC network, the output voltage and current of each DC unit will be affected when

a short-circuit fault occurs at any point on the DC line. Not only the units at both ends of the fault line feed power to the fault point, but the other non-faulted DC terminals also feed power to the fault point via the corresponding line. The voltage and current changes hugely while the fault characteristics of the voltage and current at the end of the wrong line and the non-faulted line are similar. The voltage and current changes severely at the fault line while the amplitude of voltage and current changes slightly at the non-faulted line. Fig.1 is an equivalent circuit diagram of the faulty part in case of the system has a ground fault. The protection device would be installed at both ends of each line. The system issues an order to trip when the failure occurs in a particular line; at the same time the protection devices at both ends of the line act to remove the faulty line.

Another possibility is to utilize the current change rate to detect the fault. Each DC breaker has an inductor in series with it to limit the current rise rate. The rate of change of current is given by,

$$\frac{di}{dt} = \frac{v_C(t) - v_R(t)}{L} \tag{1}$$

The fault circuit shown in Fig. 4 is simulated. When a fault occurs at F_1, as shown in Fig. 2(a), the line voltage v_R rapidly drops to a specific value, and the busbar voltage v_C falls at a relatively moderate rate in a few microseconds due to the presence of the finite current inductance. When a fault occurs at F_2, as shown in Fig. 2(b), both the line side voltage v_R and the bus voltage v_C are slowly decreasing, but the busbar voltage v_C is falling fast. As can be seen in Fig. 2, F_1 fails, $v_C > v_R$. F_2 fails, $v_C < v_R$.

3. PREDICTED VOLTAGE

In this paper, the voltage variation on the line side of the protection device is used to identify and cut off the fault, which is based on the difference between the predicted voltage and the measured voltage on the line side. It can be seen from the literature that DC is a quadratic function related to time, so the DC voltage $v_R(t)$ is also a quadratic function related to time. The voltage second derivative related to time is a constant, so,

$$\frac{dv_R^2(t)}{t^2} = \frac{dv_R^2(t-1)}{t^2} \tag{2}$$

$$v_R(t) - 2v_R(t-1) + v_R(t-2) = v_R(t-1) - 2v_R(t-2) + v_R(t-3) \tag{3}$$

$$v_R(t) - 3v_R(t-1) + 3v_R(t-2) + v_R(t-3) = 0 \tag{4}$$

From the voltage values of the first three sampling points, the voltage value at the next moment can be predicted.

$$v_{RP}(t) = 3v_R(t-1) - 3v_R(t-2) + v_R(t-3) \tag{5}$$

To verify the fitting effect of the predicted voltage and the actual voltage, a DC ring distribution network as shown in Fig. 3 is constructed. The parameters are shown in Table 1. The DC system is in a buck operation state, and its control strategy follows the master-slave control model, VSC1 controls the DC voltage of the entire network, VSC2、VSC3 and VSC4 control the power transmission.

Table 1 Parameters of Ring DC distribution network

DC Grid Voltage /kV	1.5	VSC1	0.5MW
Cable Resistance mΩ/km	10	VSC2	1MW
Cable Inductance μH/km	10	VSC3	2MW
Filter Capacitor /mF	25	VSC4	2MW

In the normal operation of the system, the power flow is changed, and the collected voltage variation curve is shown in Fig. 4. As can be seen from the figure, vRP is highly fitted to v_R as power changes. Fig. 5 is a waveform diagram showing the difference between the predicted voltage and the measured voltage on the line side at the time of failure at F_1.

4. PROTECTION STRATEGY

4.1. Staring Criterion

In the ring DC distribution network, the DC link capacitor discharges through the DC line in case of DC failure, it could lead to a large inrush DC. So the overcurrent protection can be used as the starting component. The starting component acts as a fault alarm which indicates the occurrence of faults, and the fault location algorithm begins to run once the starting component is activated. The overcurrent protection criterion is given as equation (6).

$$\left|i_{cable}\right| > i_{set} \tag{6}$$

Although adopting a smaller set may benefit for fault detection while even weak feature fault can be detected quickly. However, i_{set} cannot be set too small lest frequently tripping because of the disturbance of noise. In this paper, i_{set} in the equation (6) equals $1.2I_N$ so the starting criterion can be tripped, and the weakest fault at the end of the line can be detected. I_N is the rated current of the cable.

4.2. Primary protection criterion

It can be seen from Fig. 4 that when the system is in normal operation, the difference between the predicted voltage and the measured voltage is zero; when the DC line fails, the difference between the predicted voltage and the measured voltage on the line side is not zero. For studying the change of voltage difference and the influence on adjacent lines in the DC line fault of the toroidal DC distribution network, the faults are set in the positions of F_1, F_2, F_3 and F_4 as shown in the figure, and changed. The transition resistance, the simulation results are shown in Fig.6 and Fig.7.

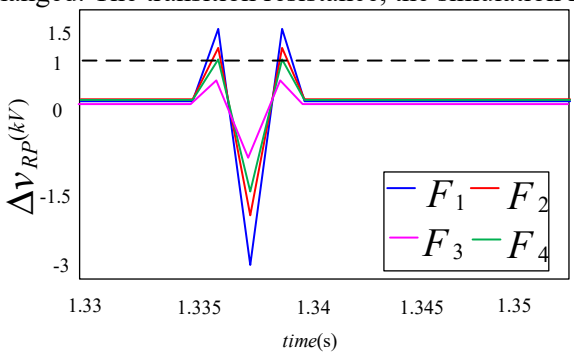

Fig.6. Variations in voltage difference detected at $PD_{1,2}$ when a metal ground fault occurs in F_1, F_2, F_3, and F_4

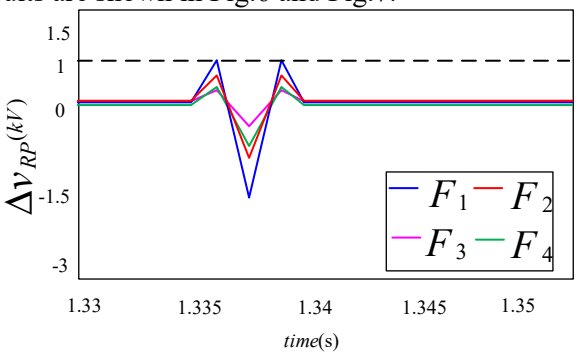

Fig.7. Variations in voltage difference detected at $PD_{1,2}$ when a high-impedance ground fault occurs in F_1, F_2, F_3, F_4

Fig.6 is a graph showing changes in the voltage difference detected at the protection devices $PD_{1,2}$ when a direct-ground short-circuit fault occurs at F_1 to F_4. Fig. 7 is a graph showing changes in the voltage difference detected at $PD_{1,2}$ when a grounding resistance short circuit occurs at F_1 to F_4. As can be seen from the figure, there is a significant difference between the predicted voltage and the measured voltage in the event of a fault. Due to the small cable impedance of the DC grid and the large filter capacitance, the current rises very fast, resulting in a huge voltage drop in the voltage. Since the predicted voltage is calculated based on the voltage of three consecutive sampling moments during normal operation of the system. When the fault occurs, the predicted voltage is still the voltage during normal operation of the system, and the measured voltage is the fault voltage, so the predicted voltage and measured The voltage will have a significant difference when the fault occurs. The difference between the predicted voltage and the actual voltage depends on the network and fault parameters such as fault resistance and fault location. It can be seen from Fig. 5 that the difference between the predicted voltage and the measured voltage is different for the fault location. The instantaneous fault voltage and the measured voltage difference at F_1 are close to 1.5kV, and the voltage difference at F_3 is only 0.3kV. Comparing Fig. 6 and Fig. 7, it can be seen that as the transition

resistance increases, the difference between the predicted voltage and the measured voltage also decreases. The most important thing is that comparing the F_2 fault of Fig.6 with the F_1 fault of Fig.7, it can be seen that the predicted voltage and the measured voltage difference are the same, but the difference between the former is higher than the latter.

To solve this problem, this paper has set the difference between the predicted voltage and the measured voltage. The protection criteria are shown in the equations (7) and (8).

$$\Delta v_{RP} = v_{RP} - v_R \tag{7}$$

$$\Delta v_{\min} \le \Delta v_{RP} \le \Delta v_{\max} \tag{8}$$

In Fig.1, when a fault occurs at F1, the voltage detected at the sampling point is given as equation (9).

$$v_R = l\frac{di}{dt} + ir + v_F \tag{9}$$

Substituting equation (9) into equation (7),

$$\Delta v_{RP} = v_{RP} - l\frac{di}{dt} - ir - v_F \tag{10}$$

In the distribution network, the resistance and inductance of the cable are minimal. The fault current does not rise at the moment of the fault due to the presence of the current limiting inductor, so the influence of the line inductance and resistance on the line side voltage is negligible. Equation (18) can be simplified,

$$\Delta v_{RP} = v_{RP} - v_F \tag{11}$$

Therefore, the setting value depends on the predicted voltage value and the fault point voltage. When a direct ground fault happens, the fault voltage is zero at the fault point. Setting the line side voltage is 1p.u during system normal operating. So, the previously sampled data v_R(t-1) to v_R(t-3) are 1pu. As a result, v_{RP} becomes 1pu, which results in $v_{\max}$=1pu.

When a high-impedance ground fault, the protection needs to avoid direct ground short circuit on the adjacent line lest causing the maximum voltage difference. From Fig. 4, the line side voltage of the line is as shown in the equation (12).

$$v_{R1} = v_C + L\frac{di_2}{dt} \tag{12}$$

Substituting equation (12) into equation (7),

$$\Delta v_{RP} = v_{RP} - v_C - L\frac{di_2}{dt} \tag{13}$$

$$\Delta v_{\min} = \frac{\Delta v_{RP}}{1.5 \times 1.1} \tag{14}$$

1.1 is the reliability factor, mainly considering the influence of factors such as calculation error and margin.

4.3. Backup protection criteria

The high voltage level is maintained on the line when the high-impedance ground fault happens, and the measured voltage is similar to the ring grid voltage on the line. The difference between the predicted voltage and the measured voltage is lower than the limit of the protection, and the protection will be refused. Therefore, backup protection is needed. In this paper, the under voltage protection is used as backup protection. The protection criterion is shown in formula (15).

$$|U| \le U_{set} \tag{15}$$

However, both the line and the adjacent line may detect the fault in case of high-impedance ground short-circuit fault, and it would cause a protection malfunction. Therefore, this paper adds an additional criterion. when the line fails, $v_C > v_R$. When the adjacent line fails, $v_C < v_R$. The protection criteria flow chart is shown in Fig. 8.

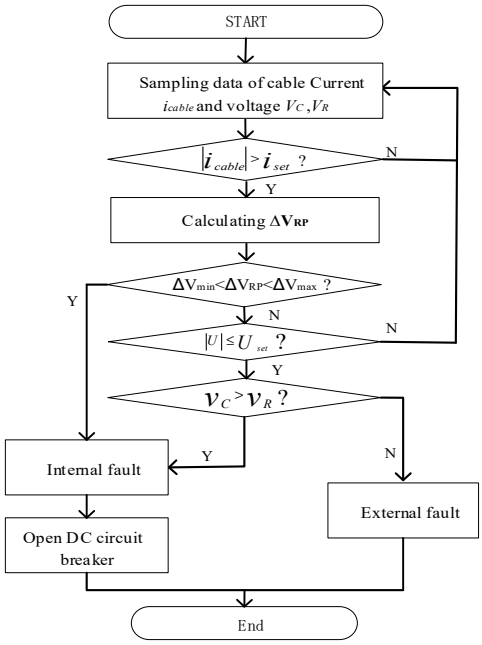

Fig.8. Flowchart of the proposed protection method

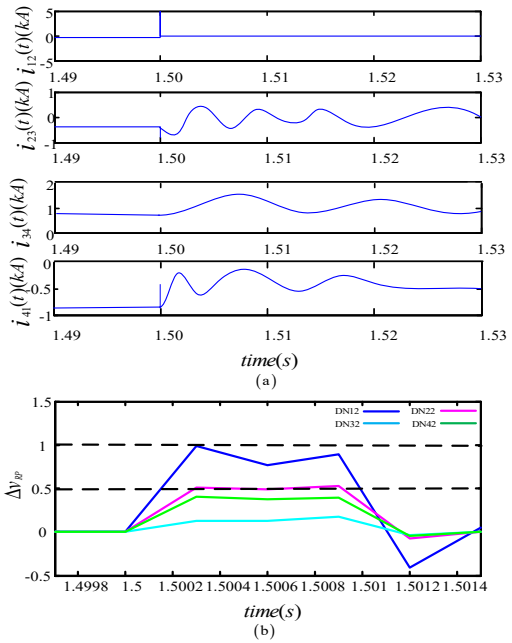

Fig.9. Variations in voltage difference detected at $PD_{1,2}$

5. SIMULATION

To verify the feasibility of the protection scheme, a four-port ring test system is built on the RTDS, as shown in Fig 3. Substituting the parameters of Table 1 into formula (13), the voltage difference that satisfies the condition is 0.825 kV. The circuit is shown in Fig. 3 is simulated, the line side voltages of adjacent lines are recorded and compared when a direct ground fault occurs at F_1 to F_4, selecting the maximum value among the minimum values. After comparison, the line voltage that meets the conditions is 0.83kV, which is consistent with the calculated line voltage value. So, Δv_{min} is 0.5 pu, the main protection setting value ranges from 0.5p.u to 1p.u.

5.1. Direct earth fault

Large filter capacitor discharge through a small R_F causes the line current i_{12} to reach to 5kA before the activation of the PD in case of a direct ground fault. As a result, the protection criteria are activated. The failure is detected within 5ms, which ensures that the system does not enter into the second stage of fault. The protective device connected to the cable continuously samples the line voltage and monitors the voltage change. As the fault F_1 occurs, calculating Δv_{RP} by the measured voltage and predicted voltage, which compared to the threshold of the protection criteria and generated a trip signal for their respective PDs. $PD_{1.2}$ and $PD_{2.1}$ to isolate the faulted line, thereby restoring the system, as shown in Fig.9.

To further test the reliability and consistency of the solution, faults at F_3 are simulated, as shown in Fig.10.

5.2. Fault with R_F

To verify the impact of RF, this paper introduces R_F=0.8Ω into the test system and tests the ground fault F_1. Other operating conditions and fault locations are the same as in the previous case. The simulation results are shown in Figure 11.

When the system fails, the line current i_{12} reaches 2kA instantaneously. As the transition resistance increasing, the adjacent line current i_{23} changes slowly and all non-faulted lines change in the same trend. The voltage difference DN12 detected by the protection device $PD_{1.2}$ has just exceeded the lower limit value, and the main protection action is performed to cut off the faulty line.

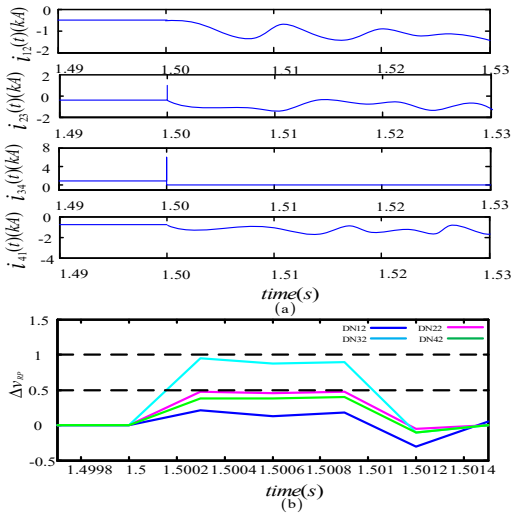

Fig.10.Currents and voltage differences of F_3

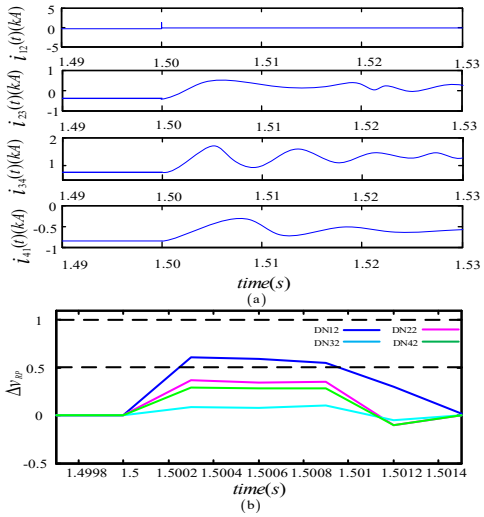

Fig.11.Currents and voltage differences of high-impedance ground fault

6. Conclusion

An effective protection system scheme for a DC distribution network has been proposed in this paper. The characteristics of the voltage at the fault point is studied and using the time-dependent quadratic model to simulate the voltage. The scheme is based on the local measurements and does not require any communication to detect the fault in the system. In this paper, the influence of ground resistance is considered comprehensively; the overcurrent protection is proposed as the starting criterion for the total protection criterion and the under voltage protection is used as backup protection. The proposed protection scheme has been verified in a toroidal DC distribution network. The proposed scheme is fast in detecting and isolating the faulty section.

Acknowledgments

Shanxi Province Key projects of Key Research and Development Program (201603D112001)

References

[1] DU Yi, JIANG Daozhuo, YIN Rui, et al. Topological structure and control strategy of the DC distribution network [J].*Electric Power Automation Equipment*,2015,35(1): 139-145.

[2] YU Xiuyong, XIAO Liye, LIN Liangzhen, et al. Single-ended Fast Fault Detection Scheme for MMC-based HVDC [J] . *High Voltage Engineering*, 2018, 44 (2) : 440-447.

[3] WEN Jialiang, WU Rui, PENG Chang, et al. Analysis of DC grid prospects in China [J]. *Proceedings of the CSEE*. 2012.32(13):7-12.

[4] CAI Zexiang, LI Jiaman, YU Chaoyun, et al. Impact of DC Disturbances on AC Protective Relaying Dynamic Behavior [J] . *High Voltage Engineering*, 2016, 10 (42) : 3246-3252.

[5] DAI Zhihui, GE Hongbo, Peter Crossley, et al. An Overview on Fault Detection and Isolation Strategies of Flexible DC Distribution Networks [J]. *Journal of North China Electric Power University*. 2017,44（4）:19-28.

[6] J. Rafferty, L. Xu, and D. J. Morrow, “DC Fault Analysis of VSC based Multi-Terminal HVDC Systems,” *in 10th IET International Conference on AC and DC Power Transmission* (ACDC 2012), 4-5 Dec. 2012, Stevenage, UK, 2012, p. 6 pp.

[7] Sneath J, Rajapakse A D., "Fault Detection and Interruption in an Earthed HVDC Grid using ROCOV and Hybrid DC Breakers," *IEEE Trans, Power Del*., vol. 31, no.3, pp. 973-981, Jun. 2016.

[8] WANG Yi, Yu Ming, ZHANG Rongli, et al. Short circuit fault analysis and protection scheme for looped DC microgrid [J]. *Electric Power Automation Equipment*，2017,37（2）：7-14.

[9] HAN Kunlun, CAI Zexiang, XU Min, et al. Dynamic Characteristics of Characteristic Parameters of Traveling Wave Protection for HVDC Transmission Line and Their Setting [J]. *Power System Technology*. 2013,37（1）:254-260.

[10] A. Meghwani, S. Srivastava, and S. Chakrabarti, “A new protection scheme for DC microgrid using current line derivative," in Proc.*IEEE/PES General Meeting*, 2015, pp. 1–5.

[11] A. Maeghwani, S. Srivastava, and S. Chakrabarti, “A non-unit protection scheme for DC microgrid based on local measurements,” *IEEE Trans.Power Del*., 2016.